Vol. 636: 107–121, 2020
https://doi.org/10.3354/meps13221

MARINE ECOLOGY PROGRESS SERIES
Mar Ecol Prog Ser

Published February 20

Evidence for inter- and intraspecific trophic niche separation among deepwater elasmobranchs on the southern Great Barrier Reef, Australia

Samantha E. M. Munroe[1,*], Cassandra L. Rigby[2], Nigel E. Hussey[3]

[1]TERN (Terrestrial Ecosystem Research Network), School of Biological Sciences, Faculty of Sciences, University of Adelaide, Adelaide, SA 5005, Australia

[2]College of Science and Engineering, Centre for Sustainable Tropical Fisheries and Aquaculture, James Cook University, QLD 4811, Australia

[3]Department of Integrative Biology, University of Windsor, 401 Sunset Avenue, Windsor, ON N9B 3P4, Canada

ABSTRACT: Quantifying the trophic structure and interactions of deepwater (>200 m depth) elasmobranch assemblages is required to improve our understanding of deepwater ecosystems and the impacts of increased deepwater exploitation. To this end, we investigated the trophic ecology of deepwater elasmobranchs on the Great Barrier Reef (GBR) using a stable isotope ($\delta^{13}C$ and $\delta^{15}N$) approach. Our study included 4 species captured in the southern GBR deepwater eastern king prawn trawl fishery: the eastern spotted gummy shark *Mustelus walkeri*, the piked spurdog *Squalus megalops*, the pale spotted catshark *Asymbolus pallidus*, and the Argus skate *Dentiraja polyommata*. The $\delta^{13}C$ and $\delta^{15}N$ values of all 4 species ranged from −18.6 to −16.2‰ and 8.3 to 13.8‰, respectively. The small $\delta^{13}C$ range was likely due to the limited number of unique carbon baseline sources typically found in deepwater environments. Despite this, 3 of the 4 species exhibited relatively low core (40% SEA_b) isotopic niche overlap (<1 to 44%). Isotopic niche separation may be driven by multiple interacting factors including morphology, feeding strategies, or resource partitioning to reduce competition. Isotope analysis also provided evidence for intraspecific variation; *S. megalops, D. polyommata* and *M. walkeri* exhibited significant increases in $\delta^{15}N$ (~3‰) and $\delta^{13}C$ (~2‰) with size. Latitude, longitude, and depth had statistically significant but comparatively minor effects on isotope values (≤1‰) of the 4 species. Cumulatively, our results indicate that isotopic variation among deepwater elasmobranchs on the GBR is principally driven by size and species-level differences in resource use.

KEY WORDS: Elasmobranchs · Deepwater · Stable isotope analysis · Great Barrier Reef

1. INTRODUCTION

Elasmobranchs are meso- and top-level predators that play a key role in maintaining nutrient flow and community structure in global food webs (Heithaus et al. 2007, 2012, Ferretti et al. 2010). Investigations that examine the trophic ecology of elasmobranchs consequently increase our understanding of marine food web dynamics, specifically the direct and indirect effects of predator–prey interactions, and the potential impacts of population declines (e.g. Stevens et al. 2000, Kitchell et al. 2002, Hussey et al. 2015, Hammerschlag et al. 2018). Elasmobranchs are considered important predators in deepwater habitats (>200 m); however, their dietary patterns have received relatively limited scientific attention compared to those of species predominantly inhabiting the photic zone (Shipley et al. 2018). This is primarily due to the intrinsic difficulty of studying remote and difficult to access species. Nonetheless, our comparatively poor understanding of deepwater elasmobranch ecology may

*Corresponding author: samantha.munroe@adelaide.edu.au

hamper effective elasmobranch management and conservation.

Deepwater elasmobranchs are particularly vulnerable to overfishing and habitat decline because they generally grow slowly, mature late, and have few young, resulting in low biological productivity and low recovery rates (Dulvy & Forrest 2010, Kyne & Simpfendorfer 2010, Rigby & Simpfendorfer 2015). Historically, deepwater elasmobranchs were not technically accessible to most fisheries, but commercial operations are now expanding into these poorly studied habitats, raising concerns over species' abilities to withstand increased fishing pressure (Haedrich et al. 2001, Morato et al. 2006, Norse et al. 2012). Insight into the trophic structure of deepwater elasmobranch assemblages will not only improve our overall understanding of deepwater ecosystems, but may also help identify and manage the potential consequences of increased deepwater exploitation (Rombouts et al. 2013).

As a functional group, deepwater elasmobranchs display a range of feeding patterns (Dunn et al. 2010, Valls et al. 2011, Churchill et al. 2015, Shipley et al. 2017a), but collectively have a trophic level range that is similar to coastal species (Cortés 1999, Pethybridge et al. 2012, Dunn et al. 2013). To date, some studies have found strong evidence for intraspecific and ontogenetic variation in the diet of deepwater species (Dunn et al. 2013, Valls et al. 2017), but contrasting trends have also been observed. For example, Navarro et al. (2014) reported that the diet of the kitefin shark *Dalatias licha* in the Mediterranean Sea was independent of both sex and maturity. Trophic niche size and niche overlap comparisons within elasmobranch assemblages have also yielded variable results. It has been suggested that due to relatively low resource availability in most deepwater systems, species may reduce competition by using distinct dietary or spatial resources (Carrassón & Cartes 2002, Fock et al. 2002, Preciado et al. 2017). However, while some deepwater elasmobranchs exhibit unique trophic niches that are suggestive of resource partitioning (e.g. Yemisken et al. 2019), others exhibit relatively high dietary overlap and consume similar prey (e.g. Barría et al. 2018). Given the apparent diversity in dietary patterns, more work is needed to better understand the trophic structure of deepwater environments.

Stable isotope analysis (SIA) provides a valuable tool to examine the long-term trophic interactions and structure of deepwater communities (Churchill et al. 2015, Kiszka et al. 2015, Shipley et al. 2017a,b). The premise of SIA is that stable isotope (SI) values of consumers reflect the proportional contributions of the prey they consume, and can therefore be used to examine and compare consumer resource use patterns at the individual and population level (Bearhop et al. 2004, Matich et al. 2011). The $\delta^{15}N$ values of consumer tissues undergo predictable enrichment at each trophic level (from 2.2 to 3.4‰ per trophic level; Caut et al. 2009, Hussey et al. 2010, 2014, Olin et al. 2013) and are predominantly used to estimate trophic position and food web length (Speed et al. 2012, Malpica-Cruz et al. 2013, Ferreira et al. 2017). In contrast, $\delta^{13}C$ values vary markedly between different primary producers and foraging habitats (Peterson & Fry 1987, Bouillon et al. 2011), but undergo minimal trophic fractionation (from ~0.5 to 1‰; Hussey et al. 2010, Kim et al. 2012a). As a result, $\delta^{13}C$ is used to determine the range of carbon sources (e.g. prey, habitats) that contribute to consumer diet (e.g. Heithaus et al. 2013, Burgess et al. 2016). Elasmobranch muscle tissue SI values reflect shark and ray diet over relatively long periods of time (6 mo to 1 yr; Logan & Lutcavage 2010, Kim et al. 2012b); therefore elasmobranch muscle values can be used to study their average, long-term resource use patterns and overall role in aquatic ecosystems (Ramos & González-Solís 2012, Munroe et al. 2018). Although SIA provides limited taxonomic resolution compared to stomach content analysis (e.g. Nielsen et al. 2019), it is a highly useful technique to establish the ecological structure of deepwater assemblages.

The Great Barrier Reef (GBR) World Heritage Area (Queensland, Australia) is best known for its shallow water (<35 m) coral reef ecosystem. However, approximately 1/3 of the World Heritage Area is in waters deeper than 200 m and contains a diverse, abundant, but poorly studied assemblage of species (Pitcher et al. 2007, Sih et al. 2017). Within the GBR, deepwater elasmobranchs are mostly encountered as bycatch in deepwater prawn trawl and line fisheries (Patterson et al. 2018). The most commonly observed species in the eastern king prawn (EKP) trawl fishery sector around Swain Reefs in the southern GBR are the Argus skate *Dentiraja polyommata*, the piked spurdog *Squalus megalops*, the pale spotted catshark *Asymbolus pallidus*, and the eastern spotted gummy shark *Mustelus walkeri* (Rigby et al. 2016b). These species are generally small bodied, with estimated maximum total lengths ranging from 470 mm for *A. pallidus* to 1120 mm for *M. walkeri* (Last & Stevens 2009). Currently, fishing effort across the Queensland range of these species is relatively low and they are not considered at high risk of overexploitation, but catch levels in this region are poorly quantified (Simpfendorfer et al. 2019). Notably, each species has

a relatively conservative life history and low biological productivity (Rigby et al. 2016a,b), and while 3 of these species are currently assessed as Least Concern on the IUCN Red List of Threatened Species, no scientific data are available on their population size.

To our knowledge, the present study provides the first examination of trophic interactions of elasmobranchs found in deepwater habitats on the GBR, focusing on the 4 most commonly captured species in the deepwater EKP trawl fishery. Specifically, we examined inter- and intraspecific variation in $\delta^{13}C$ and $\delta^{15}N$ values of muscle tissue as indicators of long-term resource use patterns. Species isotopic niche breadth, overlap, and relative trophic position were compared, and the effect of individual length, capture location (latitude, longitude, depth), and sex on variation in SI values was examined. As the principle bycatch observed in the deepwater EKP trawl fishery, quantifying the trophic patterns of these focal bycatch species is an important first step towards a better understanding of deepwater elasmobranchs on the GBR.

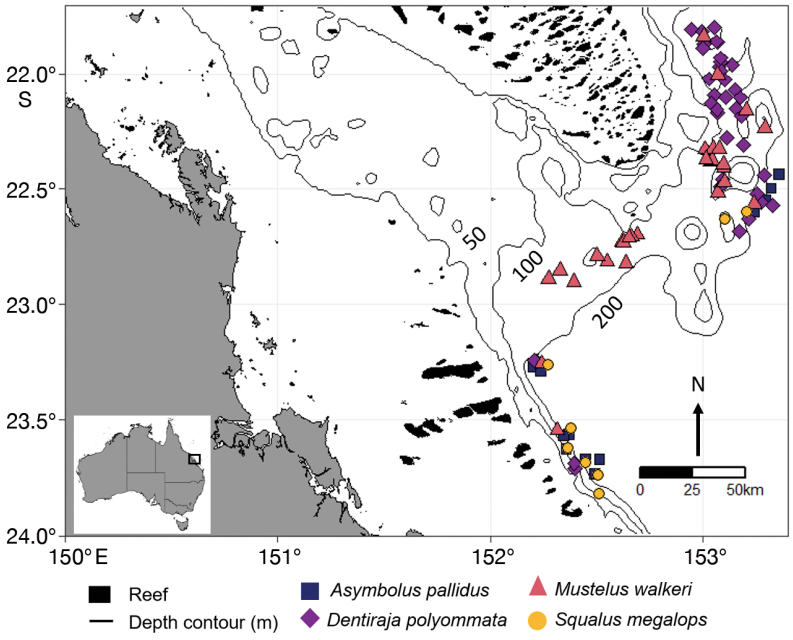

Fig. 1. Map of Swains Reef (Great Barrier Reef, Australia) and trawling locations where the 4 elasmobranch species were sampled

2. MATERIALS AND METHODS

2.1. Sample collection and stable isotope analysis

Elasmobranchs were collected from the bycatch of commercial prawn trawlers operating around Swain Reefs in the southern GBR in the deepwater eastern king prawn sector (EKP) of the Queensland East Coast Otter Trawl Fishery (Fig. 1). Details about fishing gear and specimen collection procedures are described by Rigby et al. (2016b). In brief, trawl fishing gear comprised 3 otter trawl nets of 27.4 m each. Trawls were undertaken from dusk until dawn, with each trawl an average 2.5 h duration and approximate speed of 5.4 km h^{-1}. Specimens were collected during two 5-wk trips (June–July 2011, March–April 2012). Each specimen was retained and frozen whole on-board until returned to shore for processing. Gear and fishing procedures were consistent between trips and vessels.

Upon return to the laboratory, specimens were sexed and measured for either stretched total length (mm; shark) or disc width (mm; skate). Age and reproductive maturity status were also determined for each specimen (Rigby et al. 2016a). White muscle tissue (5 g wet weight) was collected from each specimen either below the first dorsal fin (shark) or from the pectoral fin (skate). Samples were rinsed 3 times with distilled H_2O, oven dried at 60°C for 48 h, and ground into a fine powder using a stainless steel ball mill grinder. Individual isotope values for between-species comparisons can be biased by potential high lipid and urea content in elasmobranch tissue (Kim & Koch 2012); urea is depleted in ^{15}N, while lipids are depleted in ^{13}C. Therefore, samples underwent lipid and urea extraction using a modified Bligh & Dyer (1959) method: 1.9 ml of 2:1 chloroform-methanol was combined with the powdered samples, the mixture was agitated for 10 s, and placed in a water bath (30°C) for 24 h. After being removed from the bath, samples were centrifuged for 3 min, decanted, and the entire process was repeated a second time. The resultant tissue pellet was left in a fume hood to dry for 48 h, and then 400–600 µg of dried elasmobranch muscle was weighed into tin cups and analysed for $\delta^{13}C$ and $\delta^{15}N$ using a continuous flow isotope ratio mass spectrometer (IRMS, Finnigan MAT Delta^{plus}, Thermo Finnigan) equipped with an elemental analyser (Costech).

SI ratios are expressed in δ notation as deviations from standards in parts per mil (‰) using the following calculation: $\delta X = [(R_{sample}/R_{standard}) - 1] \times 1000$, where X is ^{13}C or ^{15}N, R_{sample} is the ratio ($^{13}C/^{12}C$, $^{15}N/^{14}N$) in the sample, and $R_{standard}$ is the ratio in the

standard. Laboratory and National Institute of Standards and Technology (NIST) standards were used to estimate analytical precision. ^{13}C was calibrated using Vienna Pee Dee Belemnite carbonate (VPDB), ^{15}N using atmospheric N_2. The analytical precision (SD) of 4 standards (NIST1577c, internal lab standard tilapia muscle, USGS 40 and Urea) was measured as ≤0.17‰ for $\delta^{15}N$ and ≤0.19‰ for $\delta^{13}C$ across all standards. The analytical accuracy was based on certified values of USGS 40 and showed a difference of 0.09‰ for $\delta^{15}N$ and 0.01‰ for $\delta^{13}C$. Duplicate samples of a random subset of individuals were analysed as an additional measure of accuracy. The analytical accuracy for duplicates was calculated as the mean and SD of the absolute difference between each set of duplicate samples. Differences were 0.12 ± 0.11‰ and 0.14 ± 0.34‰ for $\delta^{13}C$ and $\delta^{15}N$, respectively. Sample preparation was carried out at James Cook University (Townsville, Australia) and Griffith University (Brisbane, Australia). Lipid extraction and SIA were carried out at the Great Lakes Institute for Environmental Research, University of Windsor (Windsor, Canada).

2.2. Data analysis

Species $\delta^{13}C$ and $\delta^{15}N$ values were compared using a one-way ANOVA and Tukey's post-hoc tests were used to identify pairwise differences. Isotope values were visualised using isotopic bi-plots. Bayesian standard elliptical areas (SEA_b) (Jackson et al. 2011) and convex hulls, also referred to as the total area (TA) metric (Layman et al. 2007), were used to compare the isotopic niche breadth of each species. SEA_b were fitted to include 95% and 40% of the SI values for each species with an Inverse Wishart prior and 20 000 model iterations; 95% SEA_b estimated the extent of each isotopic niche, while 40% SEA_b provided a conservative estimate of core isotopic niche breadth. Convex hulls are the smallest possible polygon that includes 100% of the isotope values (Jackson et al. 2011). Standard elliptical areas corrected for small sample size (SEA_c) and TAs were plotted to visualise the isotope niche breath of each species with SEA_c also used to calculate the proportional (%) isotopic overlap between species. Proportional overlap was calculated as the overlapping area of 2 ellipses (species A and B) divided by the area of each ellipse (species A or B). This yielded 2 values: the proportion of niche of species A that overlaps with B, and the proportion of species B niche that overlaps with A. Additional Layman metrics were also used to compare the isotopic niche structure of each species within the assemblage using individual observations (Layman et al. 2007). Mean distance to the centroid (CD) was determined for each species to compare the mean degree of trophic diversity. Mean nearest neighbour distance (NND) and the standard deviation of NND (SDNND) was used to compare the degree of individual variation. Layman metrics were calculated and elliptical analysis was performed using the R package *SIBER* (Jackson et al. 2011).

Multiple linear regressions were used to evaluate intraspecific trends in SI values. Specifically, we examined the relationship between $\delta^{13}C$ and $\delta^{15}N$ values and elasmobranch total length (or disc width), sex, trawl location (latitude and longitude), and trawl depth. Preliminary analysis indicated the year specimens were captured had no significant effect on SI values; therefore, data were pooled across years. Models were compared using Akaike information criterion with a small sample size correction (AICc) and Akaike weights. A stepwise model selection process was used to identify the best-fit model. Multicollinearity between independent variables was assessed using Variance Inflation Factors (VIF). If VIF was >2.0, the relationship between collinear variables was evaluated using a simplified linear regression. If R^2 was >0.6, the variables were considered correlated and the inclusion of both variables had the potential to bias the model. We then used a similar stepwise model comparison process to examine the effects of collinearity on coefficient estimates. If model comparisons indicated that collinear variables were leading to unreliable or unstable estimates of regression coefficients, we used AICc values to identify which variable should be removed. All models were compared to the null model using a chi-squared goodness of fit test ($p < 0.05$). Normality for all analyses in this study were assessed using qqplots. All statistical analysis was performed in the R statistical environment (R Core Development Team 2019) version 3.5.3.

3. RESULTS

A total of 182 elasmobranchs were sampled from 211 trawls across a depth range of 117 to 280 m (Rigby et al. 2016b). Sampled *Asymbolus pallidus, Dentiraja polyommata*, and *Squalus megalops* had relatively even distributions of both sexes and age classes; however, prawn trawls captured a relatively small number of mature or male *Mustelus walkeri* (Table 1). *M. walkeri*, *D. polyommata and A. pallidus* were caught across the full latitudinal and longitudi-

Table 1. Biological and catch data for 4 elasmobranch species collected for stable isotope analysis from Swains Reef, Great Barrier Reef, Australia: total number of individuals (N), number of individuals captured each year (Year; 2011/2012), mean (range) total length (*Squalus megalops*, *Asymbolus pallidus*, *Mustelus walkeri*) or disc width (*Dentiraja polyommata* (Length; mm), number of males and females (Sex), number and proportion (%) of mature individuals (Mature), and depth capture range (Depth; m)

Species	N	Year (2011/2012)	Length	Sex (M/F)	Mature	Depth
Asymbolus pallidus	44	21/23	366 (306–436)	25/19	30 (68%)	176–239
Dentiraja polyommata	46	14/21	279 (190–369)	28/25	25 (54%)	143–215
Mustelus walkeri	38	19/5	548 (410–1050)	9/29	5 (13%)	123–239
Squalus megalops	54	47/7	354 (253–505)	26/28	19 (35%)	187–274

Table 2. Mean ± SD of $\delta^{13}C$ and $\delta^{15}N$ values of 4 elasmobranch species collected from Swains Reef, Great Barrier Reef, Australia. Layman isotopic metrics and Bayesian standard elliptical areas (SEA_b, mode + 95% credibility intervals) are provided for each species. TA: total area; CD: mean distance to the centroid; NND: mean nearest neighbour distance; SDNND: standard deviation of NND

Species	Mean $\delta^{13}C$ (‰)	Mean $\delta^{15}N$ (‰)	95% SEA_b	40% SEA_b	TA	N range (‰)	C range (‰)	CD	NND	SDNND
A. pallidus	−16.9 ± 0.3	11.9 ± 0.4	2.18 (1.59–2.92)	0.35 (0.26–0.48)	1.2	1.79	1.02	0.44	0.10	0.05
D. polyommata	−17.8 ± 0.4	10.2 ± 0.7	4.02 (2.99–5.24)	0.67 (0.5–0.87)	3.2	3.7	2.0	0.68	0.14	0.16
M. walkeri	−17.0 ± 0.3	11.8 ± 0.5	2.41 (1.71–3.46)	0.40 (0.29–0.56)	1.7	2.15	1.51	0.5	0.14	0.10
S. megalops	−17.2 ± 0.4	12.2 ± 0.8	4.23 (3.23–5.56)	0.71 (0.54–0.93)	3.4	3.1	1.7	0.76	0.14	0.11

nal range of trawl locations (Fig. 1). *A. pallidus* had a relatively large latitudinal and longitudinal distribution, but were collected from the fewest unique sites. *S. megalops* were primarily collected from the most southern trawl sites (Fig. 1).

The $\delta^{13}C$ and $\delta^{15}N$ values ranged from −18.6 to −16.2‰ and from 8.3 to 13.8‰, respectively, across all 4 species. The range of $\delta^{15}N$ values indicate that the 4 elasmobranchs consumed prey across 2 to 3 trophic levels (Olin et al. 2013, Hussey et al. 2014). ANOVA indicated significant differences in isotope values between species ($\delta^{13}C$: $F_{(3,178)} = 51.45$, $p < 0.05$, $R^2 = 0.60$ and $\delta^{15}N$: $F_{(3,178)} = 92.15$, $p < 0.05$, $R^2 = 0.45$). *D. polyommata* had significantly lower $\delta^{13}C$ and $\delta^{15}N$ values than the other 3 species (Table 2, Fig. 2; see also Table S1 and Figs. S1 & S2 in the Supplement at www.int-res.com/articles/suppl/m636p107_supp.pdf). *A. pallidus*, *M. walkeri*, and *S. megalops* had similar $\delta^{13}C$ values. *S. megalops* had significantly higher $\delta^{15}N$ values than *M. walkeri*, but *S. megalops* and *A. pallidus* $\delta^{15}N$ values were not significantly different.

A. pallidus had the smallest SEA_b, TA, CD, NND, and SDNND values, indicating it occupied the smallest isotopic niche and potentially had the lowest degree of trophic diversity. In contrast, SEA_b and Laymen metrics for *D. polyommata* and *S. megalops* indicated that these species had the largest isotopic niches and potentially the highest degree of trophic diversity. Isotope niche overlap between *D. polyommata* and all other species was low for both 95% (17–45%) and 40% SEA_c (<1%; Fig. 2). The 95% SEA_c overlap between *S. megalops* and *M. walkeri* (50–88%) and *A. pallidus* (41–80%)

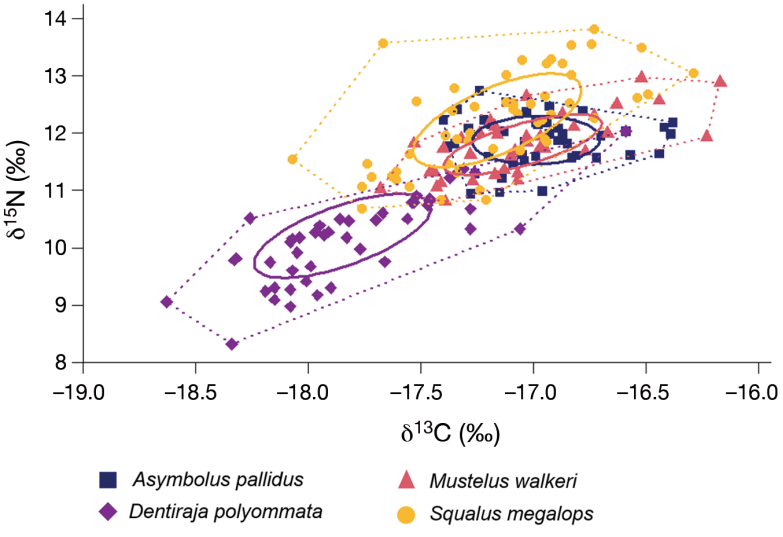

Fig. 2. Elasmobranch $\delta^{13}C$ and $\delta^{15}N$ isotope bi-plot for the 4 species (3 sharks and 1 skate) collected from Swains Reef. Standard elliptical areas (SEA_c; solid lines) are corrected for small sample size and have been fitted to the 40% core isotope values. Convex hulls (TA; dotted lines) encompass all the isotope values for each species

Table 3. Multiple linear regression model selection results for elasmobranch $\delta^{13}C$ and $\delta^{15}N$ values. Residual deviance and residual degrees of freedom (Dev/DF), Akaike's information criterion (AICc), ΔAICc, and Akaike weights (Weight) values are given for each model. The best fit models are marked by an asterisk (*). Only models with a ΔAICc < 2 were included in the table (with the exception of the null model)

Isotope	Model	Dev/DF	AICc	ΔAICc	Weight
A. pallidus					
$\delta^{13}C$	~ 1	3.18/43	16.2	18.4	0.00
	Longitude*	2.00/42	−2.0	0	0.35
	Longitude+Length	1.90/41	−1.7	0.35	0.30
	Longitude+Sex	1.97/41	−0.2	1.76	0.15
$\delta^{15}N$	~ 1	6.43/43	44.1	4.02	0.0
	Longitude*	5.45/42	40.1	0	0.31
	Length	5.60/42	41.2	1.10	0.18
	Longitude+Length	5.32/41	41.5	1.38	0.16
	Longitude+Sex	5.39/41	42.1	1.98	0.12
D. polyommata					
$\delta^{13}C$	~1	7.03/45	105.8	112.9	0.00
	Disc Width + Longitude + Sex + Depth + Disc Width × Sex*	1.62/40	−6.4	0.0	0.144
	Disc Width + Longitude + Sex + Disc Width × Sex	1.75/41	−5.7	0.77	0.98
	Disc Width + Longitude + Depth	1.88/42	−5.0	1.4	0.07
$\delta^{15}N$	~1	24.5/45	105.9	47.75	0.0
	Disc Width + Latitude + Sex+Sex × Disc Width*	7.00/41	58.1	0.0	0.14
	Disc Width + Latitude + Longitude + Sex + Sex × Disc Width	6.66/40	58.6	0.5	0.11
M. walkeri					
$\delta^{13}C$	~1	4.46/37	31.2	29.0	0.00
	Length*	1.98/36	2.2	0.0	0.47
	Length + Depth	1.93/35	3.7	1.5	0.22
	Length + Latitude	1.93/35	3.8	1.6	0.22
$\delta^{15}N$	~1	10/37	61.6	12.9	0.0
	Length + Latitude*	6.96/36	48.6	0.0	0.52
	Length	6.28/35	50.0	1.40	0.25
S. megalops					
$\delta^{13}C$	~1	7.27/53	49.2	23.17	0.00
	Length*	3.30/52	26.0	0.0	0.62
$\delta^{15}N$	~1	35.2/53	134.3	58.9	0.0
	Length*	11.3/52	75.4	0.0	0.25

was moderate, while the 40% SEA_c overlap was relatively low (~23–44% for both comparisons). Both 95% and 40% SEA_c overlap between *M. walkeri* and *A. pallidus* was high (95%: 70–77%; 40%: 69–76%).

A. pallidus $\delta^{13}C$ and $\delta^{15}N$ regression analysis identified high collinearity between latitude, longitude and depth (VIF > 3, R^2 > 0.6). Based on our model selection process, latitude and depth were excluded from both the $\delta^{13}C$ and $\delta^{15}N$ models. Results of *A. pallidus* $\delta^{13}C$ regression analysis indicated that the best fit model only included longitude as a factor ($F_{(1,42)}$ = 23.65, p < 0.05, R^2 = 0.36), with *A. pallidus* $\delta^{13}C$ values increasing with increasing longitude (Table 3, Fig. 3b). Sex and length were also included as factors in additional models with ΔAICc < 2; however, length and sex appeared to have a minimal effect on *A. pallidus* $\delta^{13}C$ values (Fig. 3a,c). The best fit model for *A. pallidus* $\delta^{15}N$ values also included longitude as a factor ($F_{(1,42)}$ = 6.52, p < 0.05, R^2 = 0.11; Fig. 3e, and length and sex were included as factors in models with a ΔAICc < 2 (Table 3, Fig. 3d,f). However, the best-fit $\delta^{15}N$ model had limited explanatory power, indicating that none of the considered variables had a strong influence on *A. pallidus* $\delta^{15}N$ values.

D. polyommata regression analysis identified collinearity between latitude and longitude (VIF > 2). However, the R^2 < 0.6, and the inclusion of both latitude and longitude did not have a notable effect on regression coefficients; therefore, no variables were removed. The best fit *D. polyommata* $\delta^{13}C$ model included disc width, longitude, depth, sex, and the interaction between sex and disc width ($F_{(3,42)}$ = 26.69, p < 0.05, R^2 = 0.74). *D. polyommata* $\delta^{13}C$ values increased with increasing disc width, and increased

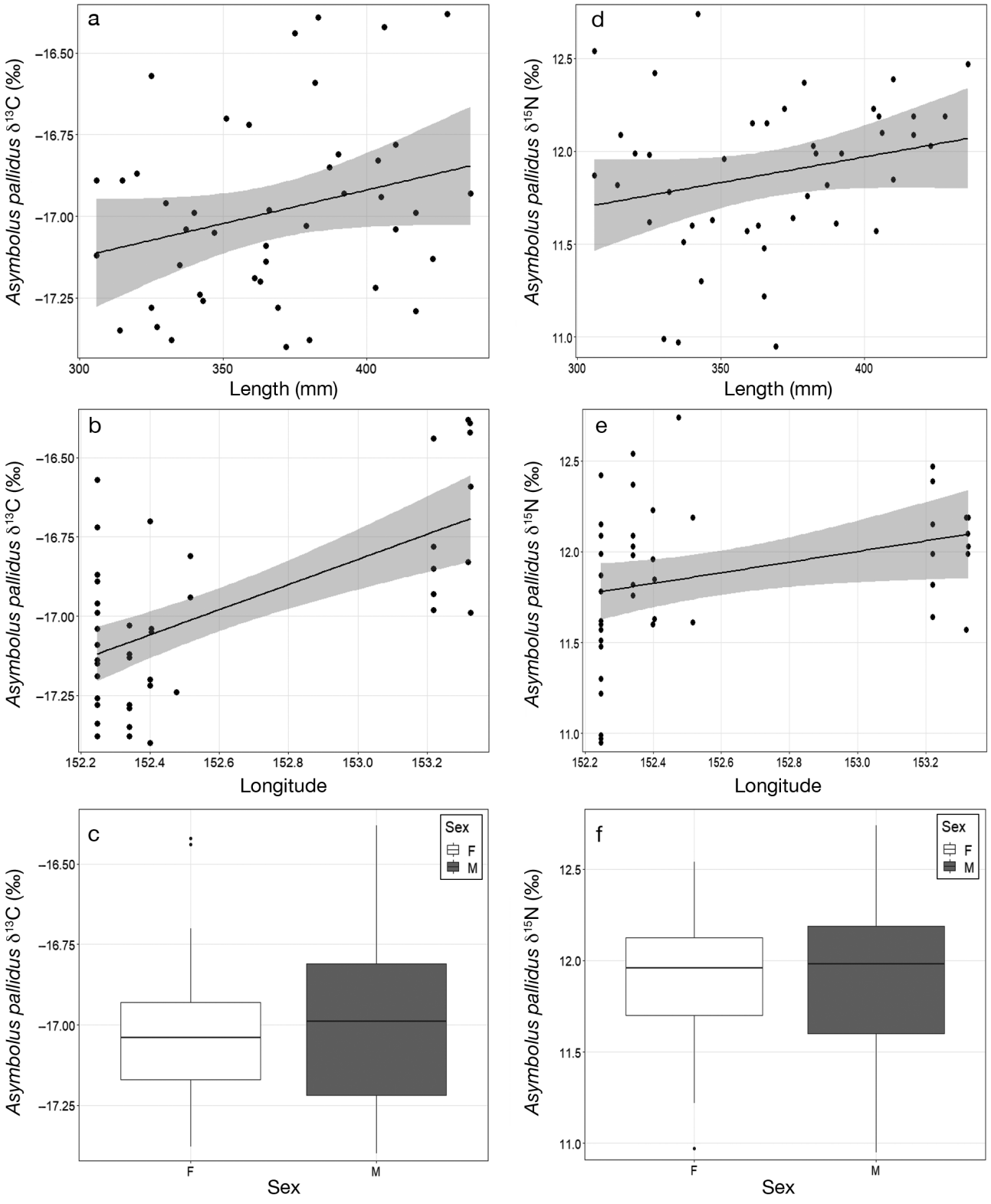

Fig. 3. Multiple linear regression model selection results for *Asymbolus pallidus* $\delta^{13}C$ and $\delta^{15}N$ values relative to (a,d) length, (b,e) longitude, and (c,f) sex. Factors were selected based on Akaike information criterion with a small sample size correction (AICc < 2). For line plots, the black lines are the predictions of the linear models, and grey bands are the 95% confidence intervals. For boxplots, the box defines the first and third quartile (likely range of variation), lines (whiskers) are the maximum and minimum range of variation, points are outliers. The middle band is the median stable isotope value

at a higher rate in males than females (Fig. 4a). *D. polyommata* $\delta^{13}C$ values decreased with increasing depth and increased with increasing longitude (Fig. 4b). The best fit *D. polyommata* $\delta^{15}N$ model included disc width, latitude, sex, and the interaction between sex and disc width ($F_{(4,41)} = 25.66$, $p < 0.05$, $R^2 = 0.68$). *D. polyommata* $\delta^{15}N$ values increased with disc width at a higher rate for males (Fig. 4d), and decreased with decreasing latitude (Fig. 4e). However, it should be noted that *D. polyommata* were predominantly captured at more narrow ranges of longitudes and latitudes than the other focal species, and highly clustered data have the potential to bias regression outputs. Sex-based trends also appeared to be driven by one male with uniquely high $\delta^{13}C$ and $\delta^{15}N$ values.

M. walkeri regression analysis identified high collinearity between latitude and longitude (VIF > 5, $R^2 = 0.78$); longitude was ultimately excluded from the $\delta^{13}C$ analysis for this species. Due to the small number of male *M. walkeri* collected, sex was also excluded. *M. walkeri* $\delta^{13}C$ regression analysis indicated the best-fit model included length as a factor ($F_{(1,36)} = 47.17$, $p < 0.05$, $R^2 = 0.54$), where $\delta^{13}C$ values increased with length (Fig. 5a). Depth and latitude were also included as factors in other *M. walkeri* $\delta^{13}C$ models with an AICc < 2. *M. walkeri* $\delta^{13}C$ values increased with increasing with latitude (Fig. 5b) and depth (Fig. 5c) but the change was small and model weights were relatively low. Based on our model selection process, the best-fit model for *M. walkeri* $\delta^{15}N$ values included length and latitude as factors ($F_{(2,35)} = 10.49$, $p < 0.05$, $R^2 = 0.33$). *M. walkeri* $\delta^{15}N$ increased with length (Fig. 5d), but the effect of latitude was relatively minor (< 1‰, Fig. 5e).

S. megalops regression analysis identified high collinearity (VIF > 7, $R^2 = 0.8$) between latitude, longitude, and depth. In addition, *S. megalops* catch distribution was clustered such that the majority of relatively small individuals (250–300 mm) were captured within a narrow latitudinal (−22.8 to −23.0°), longitudinal (153.0 to 153.25°), and depth range (190 to 210 m). Larger individuals were generally caught at deeper depths (220 to 240 m) and more southerly sites; therefore, comparisons between length and location would have confounded model interpretation. As a result, only length and sex were included in *S. megalops* $\delta^{13}C$ and $\delta^{15}N$ analysis. The best fit $\delta^{13}C$ and $\delta^{15}N$ regression models included length as a factor ($F_{(1,52)} = 31.24$, $p < 0.05$, $R^2 = 0.36$ and $F_{(1,52)} = 109.34$, $p < 0.05$, $R^2 = 0.67$, respectively) but not sex. Both $\delta^{13}C$ and $\delta^{15}N$ values increased with length in *S. megalops* (Fig. 6).

4. DISCUSSION

Deepwater environments are home to a diverse and unique array of elasmobranchs (Priede et al. 2006, Kyne & Simpfendorfer 2010, Brooks et al. 2015). Although most deepwater elasmobranchs are considered inherently vulnerable to fisheries exploitation and habitat destruction (Simpfendorfer & Kyne 2009), relatively few studies have investigated their trophic structure (e.g. Valls et al. 2011, Shipley et al. 2017b, Barría et al. 2018). In the present study, SIA was able to identify significant interspecific variation among the 4 deepwater elasmobranchs sampled from the southern GBR. Multiple species exhibited low core isotopic niche overlap, suggesting that they consume unique dietary resources. Low isotopic niche overlap is a common finding within elasmobranch assemblages (e.g. Heithaus et al. 2013, Albo-Puigserver et al. 2015, Valls et al. 2017). For example, Espinoza et al. (2015) reported low isotopic overlap among 4 sympatric elasmobranch species along the Pacific coast of Costa Rica, which in combination with stomach content analysis strongly indicated that these species targeted unique prey and/or spatial habitat resources. Competition for habitat and prey can be a key limiting factor for animal growth and survival (McMahon & Tash 1988, Webster 2004, Benkwitt 2013). Given that deepwater systems often have low resource availability, elasmobranchs may partition resources to reduce competition and increase productivity, enabling long-term co-existence (Barría et al. 2015, Pardo et al. 2015). In agreement, Dunn et al. (2013) found that the diets (identified from stomach contents) of 11 deepwater squaliform shark species, caught across the Chatham Rise in New Zealand, were highly variable in terms of prey consumed. Species also exhibited different depth and location preferences. Dunn et al. (2013) suggested these results were congruous with niche differentiation to reduce interspecific competition. While the present study focused on only 4 elasmobranch species that are part of a much larger GBR predator community (Chin et al. 2010, Rigby et al. 2016b), our results indicate that resource partitioning may help support the continuing co-existence of deepwater elasmobranch assemblages.

Interspecific variation in isotope values was also likely driven by differences in morphology, feeding strategies, and habitat use. For example, *Dentiraja polyommata* exhibited negligible isotopic overlap with the 3 other species, had the lowest $\delta^{13}C$ and $\delta^{15}N$ values, and the highest degree of trophic diversity as identified by Layman metrics. Cumulatively, these

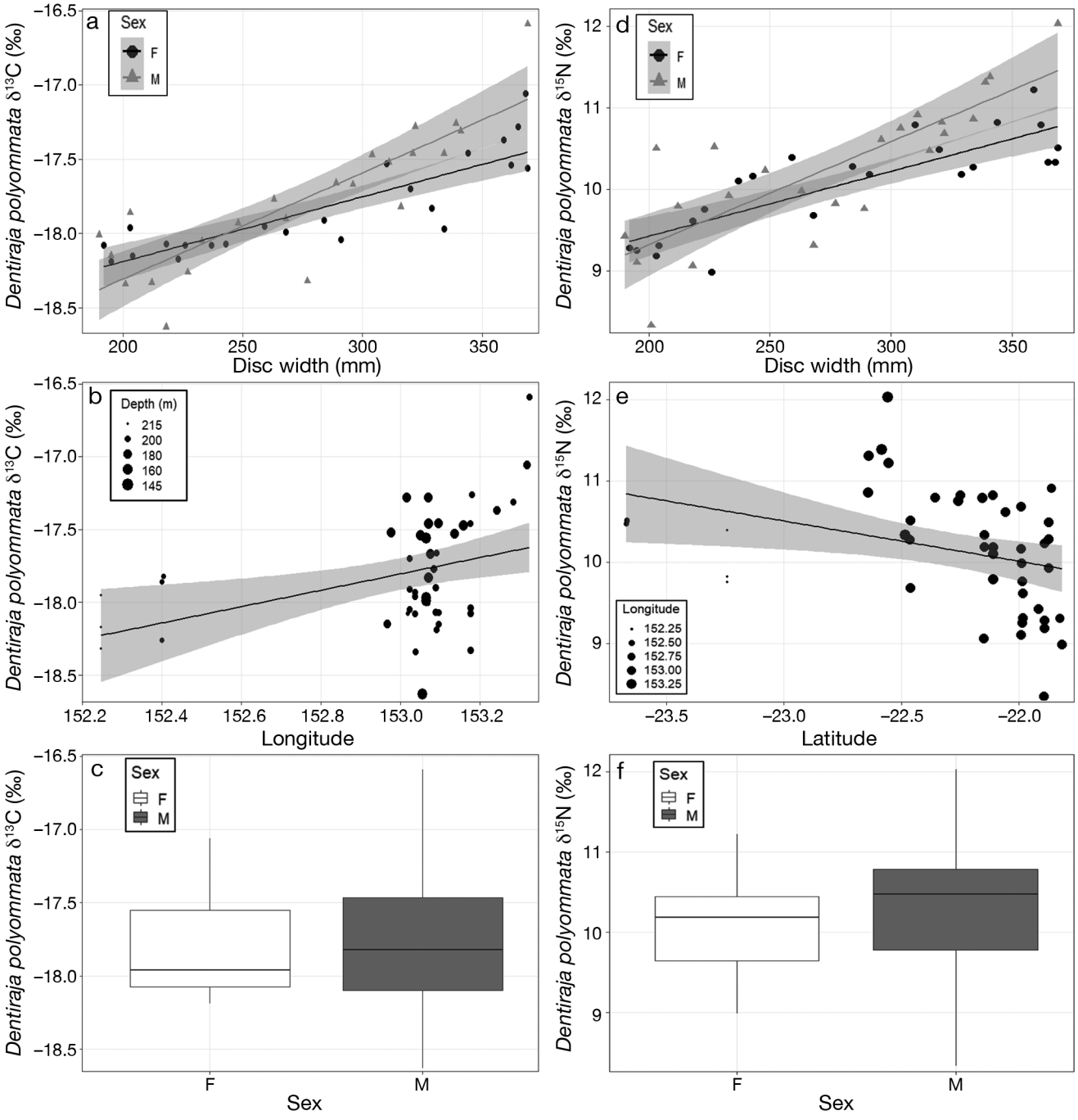

Fig. 4. Multiple linear regression model selection results for *Dentiraja polyommata* $\delta^{13}C$ and $\delta^{15}N$ values relative to (a,d) disc width, (b,e) longitude and depth, and (c,f) sex. Factors were selected based on Akaike information criterion with a small sample size correction (AICc < 2). For line plots, the black lines are the predictions of the linear models, and grey bands are the 95% confidence intervals. For boxplots, the box defines the first and third quartile (likely range of variation), lines (whiskers) are the maximum and minimum range of variation, points are outliers. The middle band is the median stable isotope value

results indicate *D. polyommata* consumes a distinct range of lower trophic level prey (Hussey et al. 2012, Munroe et al. 2018). Our findings are supported by previous stomach content and catch data which found that *D. polyommata* feeds primarily on benthic crustaceans within a depth range of 135 to 320 m (Kyne et al. 2008, Last & Stevens 2009). As the only skate included in this study, it is likely that *D. polyommata* consumes a unique range of benthic resources compared to the 3 sharks. In contrast,

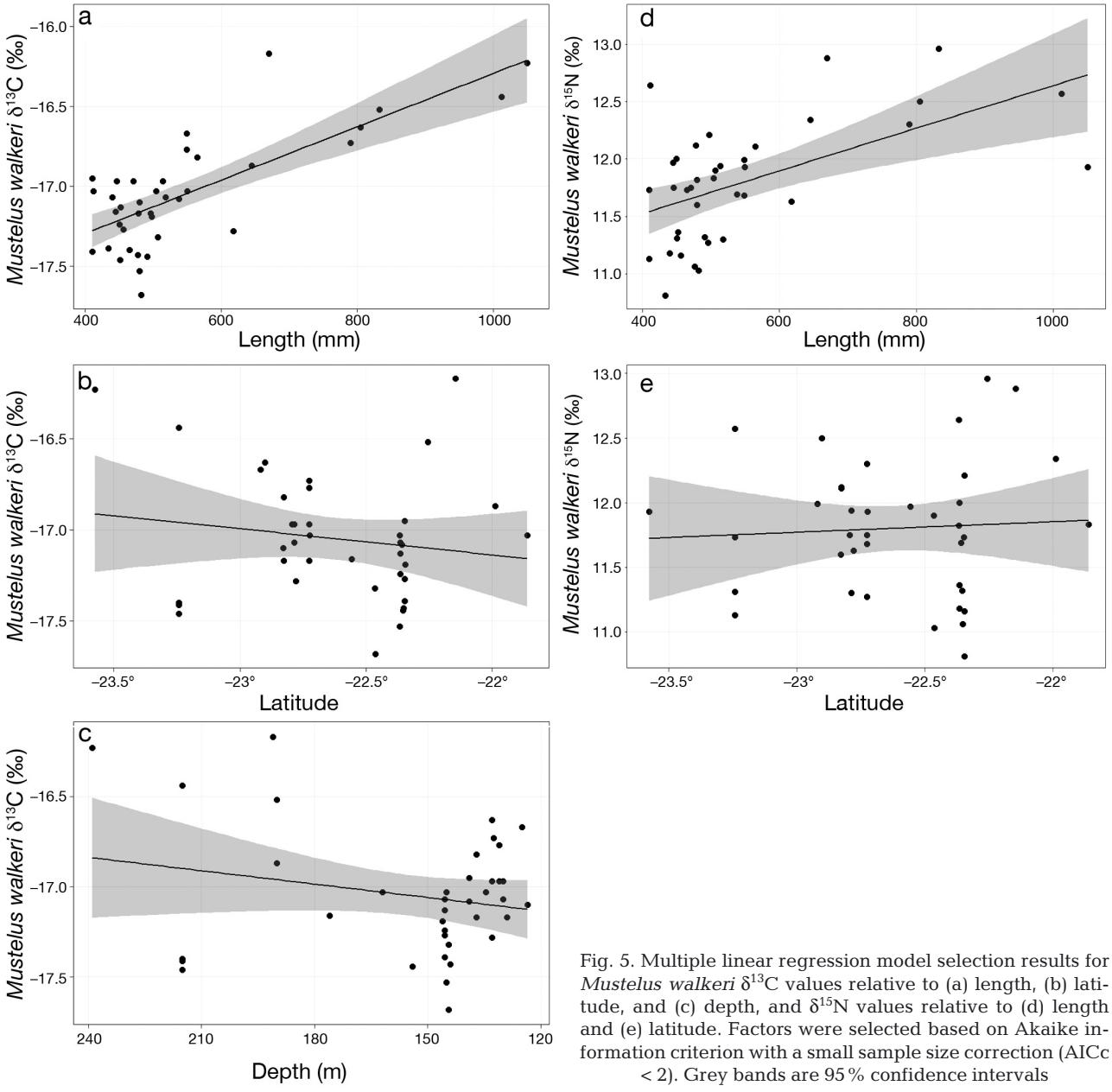

Fig. 5. Multiple linear regression model selection results for *Mustelus walkeri* $\delta^{13}C$ values relative to (a) length, (b) latitude, and (c) depth, and $\delta^{15}N$ values relative to (d) length and (e) latitude. Factors were selected based on Akaike information criterion with a small sample size correction (AICc < 2). Grey bands are 95 % confidence intervals

Squalus megalops had the highest $\delta^{13}C$ and $\delta^{15}N$ values, indicating that it consumes distinct prey at higher trophic levels. These results are consistent with *S. megalops* morphology and habitat use patterns: it has a relatively fusiform body shape and uses a wider depth range (0 to 580 m) than the other 3 species; therefore, it would likely encounter and target more pelagic/benthopelagic prey. Stomach content analysis confirms that its diet contains increased contributions of higher-level teleost prey as well as elasmobranchs (Braccini et al. 2005, Last & Stevens 2009). *Mustelus walkeri* and *Asymbolus pallidus* also had higher $\delta^{13}C$ and $\delta^{15}N$ values than *D. polyommata*, suggesting that these species also target higher trophic level prey. Our results also show that *M. walkeri* had similar $\delta^{13}C$ and lower $\delta^{15}N$ values than *S. megalops*, signifying that *M. walkeri* consume prey from similar resources pools but at a lower trophic level than *S. megalops*. Differences in $\delta^{15}N$ values could be due to *M. walkeri* morphology, which is better adapted for benthopelagic feeding, while *S. megalops* morphology targets prey throughout the water column. While it is difficult to determine the ultimate underlying causes for some of the observed trends, the distinct morphology, habitat preferences, and foraging strategies of these 4 spe-

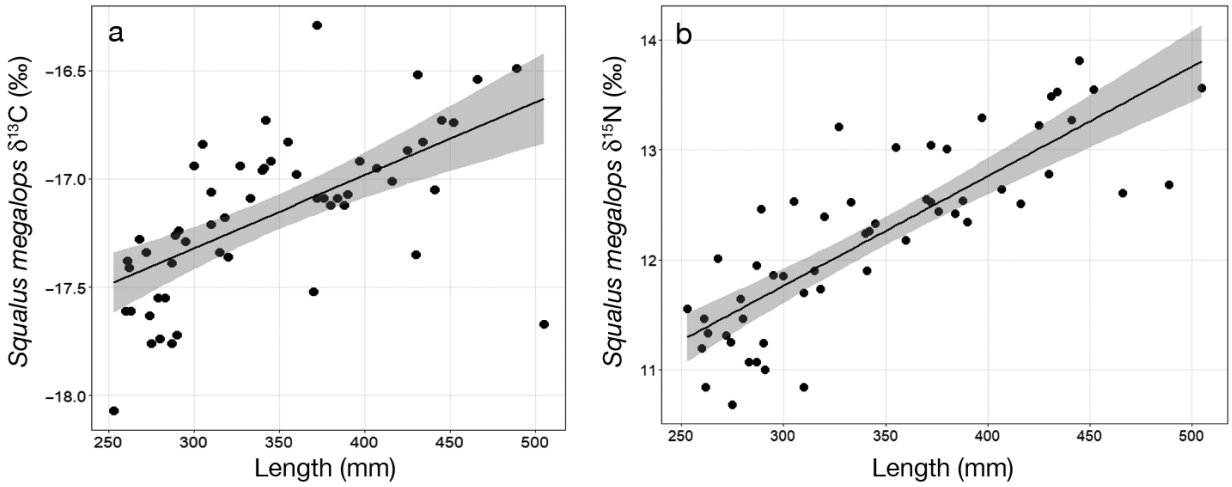

Fig. 6. Multiple linear regression model selection results for *Squalus megalops* (a) $\delta^{13}C$ and (b) $\delta^{15}N$ relative to length. Factors were selected based on Akaike information criterion with a small sample size correction (AICc < 2). Grey bands are 95% confidence intervals

cies are likely important drivers of isotopic niche separation.

While core SEA_c niche (40%) identified niche separation among species, moderate 95% SEA_c overlap values indicated that species diets were unique, but not exclusive. Specifically, high isotope niche overlap was observed between *A. pallidus* and *M. walkeri*. Previous work has found that some deepwater shark assemblages can exhibit high isotope niche overlap. For example, Barría et al. (2018) identified high overlap between 2 sympatric demersal species, the blackmouth catshark *Galeus melastomus* and the small-spotted catshark *Scyliorhinus canicula*, in the western Mediterranean Sea. Similarly, Churchill et al. (2015) reported high isotope overlap (>50%) between 7 deep-sea elasmobranchs captured over the continental shelf in the Gulf of Mexico. High isotope niche overlap could indicate that prey are a non-limiting resource between *A. pallidus* and *M. walkeri*, allowing both species to target the same prey (Vaudo & Heithaus 2011). Potentially detrimental effects of high dietary overlap could also be mitigated by predators consuming the same prey but across different depth ranges and habitats (Dunn et al. 2013, Preciado et al. 2017). *M. walkeri* is thought to use a larger and shallower depth range (53 to 403 m) than *A. pallidus* (174 to 400 m; Rigby et al. 2016b). Our results could also indicate that these species are scavenging for resources, leading to isotopic convergence (Churchill et al. 2015). Churchill et al. (2015) suggested that high isotopic overlap between deepwater elasmobranchs may also be due to the limited number of unique carbon baseline sources found in these environments, making it difficult to identify niche separation using stable isotopes alone. The $\delta^{13}C$ range observed in this study was relatively small (~3‰) compared to coastal shark communities (5 to 10‰; e.g. Papastamatiou et al. 2010, Kinney et al. 2011, Vaudo & Heithaus 2011, Heithaus et al. 2013). Therefore, while it is possible that high isotopic niche overlap between *M. walkeri* and *A. pallidus* was the result of trophic similarity, isotopic variation in this study may not comprehensively represent elasmobranch resource use patterns. Future work should incorporate stomach content and fatty acid analyses to provide more detail on relative dietary preferences of each species (Pethybridge et al. 2010, Navarro et al. 2014).

SIA also provided strong evidence for intraspecific variation among the 4 deepwater elasmobranchs examined. *D. polyommata, S. megalops,* and *M. walkeri* exhibited significant increases in isotope values with increasing length, indicating that as individuals grow they consume different (or larger) prey at potentially higher trophic levels (Hussey et al. 2011, Munroe et al. 2018). Ontogenetic variation in diet has been found in other deepwater elasmobranchs (Valls et al. 2017) and it is a relatively common finding across shark species (e.g. Bethea et al. 2006, Lucifora et al. 2009, Espinoza et al. 2012). Improved hunting ability, changes in gape and morphology, and home range expansion can all lead to a shift or increase in the range of prey available to consumers (Lowe et al. 1996, Wilga et al. 2016), resulting in a marked contrast in isotope values between juveniles and adults (Estrada et al. 2006, Malpica-Cruz et al. 2013). Different age classes may also target different resources in an attempt to limit competition, or in response to changing energetic

demands. Interestingly, *S. megalops* catch locations were also strongly clustered by size. This finding could suggest that juvenile and adult *S. megalops* segregate by depth or area (Rigby et al. 2016a), or it may signify changes in habitat use or hunting strategies with age (Afonso & Hazin 2015). In contrast to the other 3 species, there was no significant relationship between *A. pallidus* length and $\delta^{13}C$ or $\delta^{15}N$ values, indicating that their diet may be relatively consistent with size. Ontogenetic variation in diet is not always evident among elasmobranchs. For example, Shipley et al. (2018) found no ontogenetic variation in the $\delta^{13}C$ and $\delta^{15}N$ values of Atlantic chupare *Styracura schmardae* and southern stingrays *Hypanus americanus* collected from the Bahamas. However, it is important to note that no young of the year *A. pallidus* were captured in the present study, most captured individuals had already reached reproductive maturity, and *A. pallidus* size range was relatively restricted compared to the other species. Therefore, the lack of a relationship between size and $\delta^{13}C$ or $\delta^{15}N$ could be an artefact of the sample distribution.

Isotopic differences between sexes were minor in all species studied, although given the narrow isotope range found within this assemblage, it is difficult to determine if small isotopic differences between sexes are ecologically relevant. Differences between sexes were most clearly identified in *D. polyommata*, where male $\delta^{13}C$ and $\delta^{15}N$ values increased with body size at a higher rate than female values. These results could indicate that adult male and female *D. polyommata* have unique diets and use different foraging habitats. For example, Abrantes & Barnett (2011) found that female broadnose sevengill sharks *Notorynchus cepedianus* from southeast Tasmania (Australia) had relatively high $\delta^{13}C$ compared to males, suggesting that females were more closely associated with coastal habitats. Isotopic differences between sexes may also be a by-product of differences in energy and resource allocation (e.g. growth versus reproduction; Hobson et al. 2000, Martínez del Rio et al. 2009). It is important to note however that differences between male and female *D. polyommata* were heavily influenced by one male with high $\delta^{13}C$ and $\delta^{15}N$ values. Therefore, these results should be interpreted with caution and warrant further investigation.

Capture location (i.e. latitude, longitude, and depth) had a significant effect on elasmobranch isotope values; however, the effect was often small and the direction was inconsistent across species. Distinguishing the ultimate importance of latitude, longitude and depth is difficult because of the high collinearity between these factors, which was a consequence of the naturally patchy distribution of deepwater species and the clustered distribution of our fishery-dependent sampling. Nonetheless, changes in elasmobranch $\delta^{13}C$ isotope values were most strongly associated with changes in longitude, as compared to the other location variables (with the exception of *M. walkeri*). In this study, changes in longitude provide an effective proxy for distance from shelf and reef habitat. Relative proximity to shelf or reef habitats could impact prey diversity and availability, which in turn could influence elasmobranch diet and isotope values. Significant changes in elasmobranch isotope values with depth were not obvious, although this relationship has been observed in previous studies (Parzanini et al. 2017, Shipley et al. 2017b). A recent study using baited underwater cameras indicated that depth is a strong predictor of species assemblage composition in the deepwater habitats of the GBR (Sih et al. 2017), and a global analysis of deep sea shark $\delta^{13}C$ values found that shark trophic ecology is most strongly influenced by shark length and capture depth (Bird et al. 2018). The limited influence of depth on elasmobranch isotope values in this study could be due to a number of factors: (1) the small $\delta^{13}C$ range in deepwater environments (Churchill et al. 2015); (2) the fact that some species consume prey across a wide range of depths, making capture depth irrelevant when examining stable isotopes in a slow turnover tissue such as muscle; (3) the effect of length, which may have diminished the relative strength of any depth-based effects (Parzanini et al. 2017); and (4) that specimens may not have been collected over a large enough depth range to detect a strong relationship. This latter explanation is supported by the fact that the EKP trawls operate at the upper limit of the depth range of some species (90 to 300 m). For example, *A. pallidus* has a depth range of 174 to 400 m (Rigby et al. 2016b). More precise dietary and environmental information are needed to determine if deepwater elasmobranch diet changes with location, or if changes in isotope values observed in this study were indicative of changes in baseline organic sources.

Information on the trophic structure of species complexes inhabiting deepwater ecosystems is critical for an improved understanding of deepwater habitats to assist their management and conservation. Our results suggest that some deepwater elasmobranchs in the southern GBR use distinct trophic resource pools, likely due to differences in morphology and feeding strategies, and potentially as a consequence of resource partitioning. These findings

highlight the importance of maintaining intact and diverse deepwater prey communities, given that resource separation may be instrumental in supporting predators and their co-existence. Overfishing, habitat destruction, and the depletion of prey species could disrupt the ecological frameworks that support deepwater trophic structure. Fishing effort in the deepwater areas of the GBR is currently low, and deepwater species are not exposed to high fishing pressure across the majority of their range (Patterson et al. 2018, Simpfendorfer et al. 2019). However, potential plans to expand deepwater fishery operations should carefully consider the intricate trophic interactions of these systems. Future work should examine the trophic role of deepwater elasmobranchs within the larger GBR community and generate detailed deepwater environmental isotope data to contextualise subsequent research.

Acknowledgements. The authors thank the Save Our Seas Foundation and their small grant award program for supporting this research. The authors also thank S. Murphy for allowing C.L.R. onboard his company's vessels; without his and the fishers' co-operation, the samples could not have been collected.

LITERATURE CITED

Abrantes KG, Barnett A (2011) Intrapopulation variations in diet and habitat use in a marine apex predator, the broadnose sevengill shark *Notorynchus cepedianus.* Mar Ecol Prog Ser 442:133–148

Afonso AS, Hazin FH (2015) Vertical movement patterns and ontogenetic niche expansion in the tiger shark, *Galeocerdo cuvier*. PLOS ONE 10:e0116720

Albo-Puigserver M, Navarro J, Coll M, Aguzzi J, Cardona L, Sáez-Liante R (2015) Feeding ecology and trophic position of three sympatric demersal chondrichthyans in the northwestern Mediterranean. Mar Ecol Prog Ser 524: 255–268

Barría C, Coll M, Navarro J (2015) Unravelling the ecological role and trophic relationships of uncommon and threatened elasmobranchs in the western Mediterranean Sea. Mar Ecol Prog Ser 539:225–240

Barría C, Navarro J, Coll M (2018) Feeding habits of four sympatric sharks in two deep-water fishery areas of the western Mediterranean Sea. Deep Sea Res I 142:34–43

Bearhop S, Adams CE, Waldron S, Fuller RA, Macleod H (2004) Determining trophic niche width: a novel approach using stable isotope analysis. J Anim Ecol 73: 1007–1012

Benkwitt CE (2013) Density-dependent growth in invasive lionfish (*Pterois volitans*). PLOS ONE 8:e66995

Bethea D, Carlson JK, Buckel JA, Satterwhite M (2006) Ontogenetic and site-related trends in the diet of the Atlantic sharpnose shark *Rhizoprionodon terraenovae* from the northeast gulf of Mexico. Bull Mar Sci 78: 287–307

Bird CS, Veríssimo A, Magozzi S, Abrantes K and others (2018) A global perspective on the trophic geography of sharks. Nat Ecol Evol 2:299–305

Bligh EG, Dyer WJ (1959) A rapid method of total lipid extraction and purification. Can J Biochem Physiol 37: 911–917

Bouillon S, Connolly R, Gillikin D (2011) Use of stable isotopes to understand food webs and ecosystem functioning in estuaries. In: Wolanski E, McLusky D (eds) Treatise on estuarine and coastal science, Book 7. Academic Press, Waltham, MA, p 143–173

Braccini JM, Gillanders BM, Walker TI (2005) Sources of variation in the feeding ecology of the piked spurdog (*Squalus megalops*): implications for inferring predator–prey interactions from overall dietary composition. ICES J Mar Sci 62:1076–1094

Brooks EJ, Brooks AM, Williams S, Jordan LK and others (2015) First description of deep-water elasmobranch assemblages in the Exuma Sound, The Bahamas. Deep Sea Res II 115:81–91

Burgess KB, Couturier LIE, Marshall AD, Richardson AJ, Weeks SJ, Bennett MB (2016) *Manta birostris*, predator of the deep? Insight into the diet of the giant manta ray through stable isotope analysis. R Soc Open Sci 3:160717

Carrassón M, Cartes JE (2002) Trophic relationships in a Mediterranean deep-sea fish community: partition of food resources, dietary overlap and connections within the benthic boundary layer. Mar Ecol Prog Ser 241:41–55

Caut S, Angulo E, Courchamp F (2009) Variation in discrimination factors ($\delta^{15}N$ and $\delta^{13}C$): the effect of diet isotopic values and applications for diet reconstruction. J Appl Ecol 46:443–453

Chin A, Kyne PM, Walker TI, McAuley RB (2010) An integrated risk assessment for climate change: analysing the vulnerability of sharks and rays on Australia's Great Barrier Reef. Glob Change Biol 16:1936–1953

Churchill DA, Heithaus MR, Vaudo JJ, Grubbs RD, Gastrich K, Castro JI (2015) Trophic interactions of common elasmobranchs in deep-sea communities of the Gulf of Mexico revealed through stable isotope and stomach content analysis. Deep Sea Res II 115:92–102

Cortés E (1999) Standardized diet compositions and trophic levels of sharks. ICES J Mar Sci 56:707–717

Dulvy NK, Forrest RE (2010) Life histories, population dynamics and extinction risks in Chondrichthyans. In: Carrier JC, Musick JA, Heithaus MR (eds) Sharks and their relatives II: biodiversity, adaptive physiology, and conservation. CRC Press, Boca Raton, FL, p 655–696

Dunn MR, Szabo A, McVeagh MS, Smith PJ (2010) The diet of deepwater sharks and the benefits of using DNA identification of prey. Deep Sea Res I 57:923–930

Dunn MR, Stevens DW, Forman JS, Connell A (2013) Trophic interactions and distribution of some squaliforme sharks, including new diet descriptions for *Deania calcea* and *Squalus acanthias.* PLOS ONE 8:e59938

Espinoza M, Clarke TM, Villalobos-Rojas F, Wehrtmann IS (2012) Ontogenetic dietary shifts and feeding ecology of the rasptail skate *Raja velezi* and the brown smoothhound shark *Mustelus henlei* along the Pacific coast of Costa Rica, Central America. J Fish Biol 81: 1578–1595

Espinoza M, Munroe SEM, Clarke TM, Fisk AT, Wehrtmann IS (2015) Feeding ecology of common demersal elasmobranch species in the Pacific coast of Costa Rica inferred from stable isotope and stomach content analyses. J Exp Mar Biol Ecol 470:12–25

Estrada JA, Rice AN, Natanson LJ, Skomal GB (2006) Use of isotopic analysis of vertebrae in reconstructing ontogenetic feeding ecology in white sharks. Ecology 87: 829–834

Ferreira LC, Thums M, Heithaus MR, Barnett A and others (2017) The trophic role of a large marine predator, the tiger shark *Galeocerdo cuvier*. Sci Rep 7:7641

Ferretti F, Worm B, Britten GL, Heithaus MR, Lotze HK (2010) Patterns and ecosystem consequences of shark declines in the ocean. Ecol Lett 13:1055–1071

Fock HO, Matthiessen B, Zidowitz H, Westernhagen HV (2002) Diel and habitat-dependent resource utilisation by deep-sea fishes at the Great Meteor seamount: niche overlap and support for the sound scattering layer interception hypothesis. Mar Ecol Prog Ser 244:219–233

Haedrich RL, Merrett NR, O'Dea NR (2001) Can ecological knowledge catch up with deep-water fishing? A North Atlantic perspective. Fish Res 51:113–122

Hammerschlag N, Barley SC, Irschick DJ, Meeuwig JJ, Nelson ER, Meekan MG (2018) Predator declines and morphological changes in prey: evidence from coral reefs depleted of sharks. Mar Ecol Prog Ser 586:127–139

Heithaus MR, Frid A, Wirsing AJ, Dill LM and others (2007) State-dependent risk-taking by green sea turtles mediates top-down effects of tiger shark intimidation in a marine ecosystem. J Anim Ecol 76:837–844

Heithaus MR, Wirsing AJ, Dill LM (2012) The ecological importance of intact top-predator populations: a synthesis of 15 years of research in a seagrass ecosystem. Mar Freshw Res 63:1039–1050

Heithaus MR, Vaudo JJ, Kreicker S, Layman CA and others (2013) Apparent resource partitioning and trophic structure of large-bodied marine predators in a relatively pristine seagrass ecosystem. Mar Ecol Prog Ser 481:225–237

Hobson KA, Sirois J, Gloutney ML (2000) Tracing nutrient allocation to reproduction with stable isotopes: a preliminary investigation using colonial waterbirds of Great Slave Lake. Auk 117:760–774

Hussey NE, Brush J, McCarthy ID, Fisk AT (2010) $\delta^{15}N$ and $\delta^{13}C$ diet–tissue discrimination factors for large sharks under semi-controlled conditions. Comp Biochem Physiol A Mol Integr Physiol 155:445–453

Hussey NE, Dudley SFJ, McCarthy ID, Cliff G, Fisk AT (2011) Stable isotope profiles of large marine predators: viable indicators of trophic position, diet, and movement in sharks? Can J Fish Aquat Sci 68:2029–2045

Hussey NE, MacNeil MA, Olin JA, McMeans BC, Kinney MJ, Chapman DD, Fisk AT (2012) Stable isotopes and elasmobranchs: tissue types, methods, applications and assumptions. J Fish Biol 80:1449–1484

Hussey NE, MacNeil MA, McMeans BC, Olin JA and others (2014) Rescaling the trophic structure of marine food webs. Ecol Lett 17:239–250

Hussey NE, MacNeil MA, Siple MC, Popp BN, Dudley SF, Fisk AT (2015) Expanded trophic complexity among large sharks. Food Webs 4:1–7

Jackson AL, Inger R, Parnell AC, Bearhop S (2011) Comparing isotopic niche widths among and within communities: SIBER — Stable Isotope Bayesian Ellipses in R. J Anim Ecol 80:595–602

Kim SL, Koch PL (2012) Methods to collect, preserve, and prepare elasmobranch tissues for stable isotope analysis. Environ Biol Fishes 95:53–63

Kim SL, Casper DR, Galván-Magaña F, Ochoa-Díaz R, Hernández-Aguilar SB, Koch PL (2012a) Carbon and nitrogen discrimination factors for elasmobranch soft tissues based on a long-term controlled feeding study. Environ Biol Fishes 95:37–52

Kim SL, del Rio CM, Casper D, Koch PL (2012b) Isotopic incorporation rates for shark tissues from a long-term captive feeding study. J Exp Biol 215:2495–2500

Kinney M, Hussey N, Fisk A, Tobin A, Simpfendorfer C (2011) Communal or competitive? Stable isotope analysis provides evidence of resource partitioning within a communal shark nursery. Mar Ecol Prog Ser 439:263–276

Kiszka JJ, Aubail A, Hussey NE, Heithaus MR, Caurant F, Bustamante P (2015) Plasticity of trophic interactions among sharks from the oceanic south-western Indian Ocean revealed by stable isotope and mercury analyses. Deep Sea Res I 96:49–58

Kitchell JF, Essington TE, Boggs CH, Schindler DE, Walters CJ (2002) The role of sharks and longline fisheries in a pelagic ecosystem of the central Pacific. Ecosystems 5: 202–216

Kyne PM, Simpfendorfer CA (2010) Deepwater chondrichthyans. In: Carrier JC, Musick JA, Heithaus MR (eds) Sharks and their relatives II: biodiversity, adaptive physiology, and conservation. CRC Press, Boca Raton, FL, p 53–130

Kyne PM, Courtney AJ, Bennett MB (2008) Aspects of reproduction and diet of the Australian endemic skate *Dipturus polyommata* (Ogilby) (Elasmobranchii: Rajidae), by-catch of a commercial prawn trawl fishery. J Fish Biol 72:61–77

Last PR, Stevens JD (2009) Sharks and rays of Australia, 2nd edn. CSIRO Publishing, Collingwood, Victoria

Layman CA, Arrington DA, Montaña CG, Post DM (2007) Can stable isotope ratios provide for community-wide measures of trophic structure? Ecology 88:42–48

Logan JM, Lutcavage ME (2010) Stable isotope dynamics in elasmobranch fishes. Hydrobiologia 644:231–244

Lowe C, Wetherbee B, Crow G, Tester A (1996) Ontogenetic dietary shifts and feeding behavior of the tiger shark, *Galeocerdo cuvier*, in Hawaiian waters. Environ Biol Fishes 47:203–211

Lucifora L, García V, Menni R, Escalante A, Hozbor N (2009) Effects of body size, age and maturity stage on diet in a large shark: ecological and applied implications. Ecol Res 24:109–118

Malpica-Cruz L, Herzka SZ, Sosa-Nishizaki O, Escobedo-Olvera MA (2013) Tissue-specific stable isotope ratios of shortfin mako (*Isurus oxyrinchus*) and white (*Carcharodon carcharias*) sharks as indicators of size-based differences in foraging habitat and trophic level. Fish Oceanogr 22:429–445

Martínez del Rio C, Wolf N, Carleton SA, Gannes LZ (2009) Isotopic ecology ten years after a call for more laboratory experiments. Biol Rev Camb Philos Soc 84:91–111

Matich P, Heithaus MR, Layman CA (2011) Contrasting patterns of individual specialisation and trophic coupling in two marine apex predators. J Anim Ecol 80:294–305

McMahon TE, Tash JC (1988) Experimental analysis of the role of emigration in population regulation of desert pupfish. Ecology 69:1871–1883

Morato T, Watson R, Pitcher TJ, Pauly D (2006) Fishing down the deep. Fish Fish 7:24–34

Munroe S, Meyer L, Heithaus M (2018) Dietary biomarkers in shark foraging and movement ecology. In: Carrier JC, Heithaus MR, Simpfendorfer CA (eds) Shark research:

emerging technologies and applications for the field and laboratory. CRC Press, Boca Raton, FL, p 1–24
Navarro J, López L, Coll M, Barría C, Sáez-Liante R (2014) Short- and long-term importance of small sharks in the diet of the rare deep-sea shark *Dalatias licha.* Mar Biol 161:1697–1707
Nielsen J, Christiansen JS, Grønkjær P, Bushnell P and others (2019) Greenland shark (*Somniosus microcephalus*) stomach contents and stable isotope values reveal an ontogenetic dietary shift. Front Mar Sci 6:125
Norse EA, Brooke S, Cheung WWL, Clark MR and others (2012) Sustainability of deep-sea fisheries. Mar Policy 36: 307–320
Olin JA, Hussey NE, Grgicak-Mannion A, Fritts MW, Wintner SP, Fisk AT (2013) Variable $\delta^{15}N$ diet-tissue discrimination factors among sharks: implications for trophic position, diet and food web models. PLOS ONE 8:e77567
Papastamatiou YP, Friedlander AM, Caselle JE, Lowe CG (2010) Long-term movement patterns and trophic ecology of blacktip reef sharks (*Carcharhinus melanopterus*) at Palmyra Atoll. J Exp Mar Biol Ecol 386:94–102
Pardo SA, Burgess KB, Teixeira D, Bennett MB (2015) Local-scale resource partitioning by stingrays on an intertidal flat. Mar Ecol Prog Ser 533:205–218
Parzanini C, Parrish CC, Hamel JF, Mercier A (2017) Trophic ecology of a deep-sea fish assemblage in the Northwest Atlantic. Mar Biol 164:206
Patterson H, Larcombe J, Nicol S, Curtotti R (2018) Fishery status reports 2018. Australian Bureau of Agricultural and Resource Economics and Sciences, Canberra, ACT
Peterson BJ, Fry B (1987) Stable isotopes in ecosystem studies. Annu Rev Ecol Evol Syst 18:293–320
Pethybridge H, Daley R, Virtue P, Nichols P (2010) Lipid composition and partitioning of deepwater chondrichthyans: inferences of feeding ecology and distribution. Mar Biol 157:1367–1384
Pethybridge H, Butler EC, Cossa D, Daley R, Boudou A (2012) Trophic structure and biomagnification of mercury in an assemblage of deepwater chondrichthyans from southeastern Australia. Mar Ecol Prog Ser 451: 163–174
Pitcher R, Doherty P, Arnold P, Hooper J and others (2007) Seabed biodiversity on the continental shelf of the Great Barrier Reef World Heritage Area. Project Report. CRC-REEF Task Number: C1.1.2. FRDC Project Number: 2003/021. NOO Contract Number: 2004/015. Department of Primary Industries, Queensland
Preciado I, Cartes JE, Punzón A, Frutos I, López-López L, Serrano A (2017) Food web functioning of the benthopelagic community in a deep-sea seamount based on diet and stable isotope analyses. Deep Sea Res II 137:56–68
Priede IG, Froese R, Bailey DM, Bergstad OA and others (2006) The absence of sharks from abyssal regions of the world's oceans. Proc R Soc B 273:1435–1441
R Core Development Team (2019) R: a language and environment for statistical computing. R Foundation for Statistical Computing, Vienna. www.r-project.org
Ramos R, González-Solís J (2012) Trace me if you can: the use of intrinsic biogeochemical markers in marine top predators. Front Ecol Environ 10:258–266
Rigby C, Simpfendorfer CA (2015) Patterns in life history traits of deep-water chondrichthyans. Deep Sea Res II 115:30–40
Rigby CL, Daley RK, Simpfendorfer CA (2016a) Comparison of life histories of two deep-water sharks from eastern Australia: the piked spurdog and the Philippine spurdog. Mar Freshw Res 67:1546–1561
Rigby CL, White WT, Simpfendorfer CA (2016b) Deepwater chondrichthyan bycatch of the eastern king prawn fishery in the southern Great Barrier Reef, Australia. PLOS ONE 11:e0156036
Rombouts I, Beaugrand G, Fizzala X, Gaill F and others (2013) Food web indicators under the Marine Strategy Framework Directive: from complexity to simplicity? Ecol Indic 29:246–254
Shipley ON, Brooks EJ, Madigan DJ, Sweeting CJ, Grubbs RD (2017a) Stable isotope analysis in deep-sea chondrichthyans: recent challenges, ecological insights, and future directions. Rev Fish Biol Fish 27:481–497
Shipley ON, Polunina NVC, Newman SP, Sweeting CJ, Barker S, Witt MJ, Brooks EJ (2017b) Stable isotopes reveal food web dynamics of a data-poor deep-sea island slope community. Food Webs 10:22–25
Shipley ON, Murchie KJ, Frisk MG, O'Shea OR and others (2018) Trophic niche dynamics of three nearshore benthic predators in the Bahamas. Hydrobiologia 813: 177–188
Sih TL, Cappo M, Kingsford M (2017) Deep-reef fish assemblages of the Great Barrier Reef shelf-break (Australia). Sci Rep 7:10886
Simpfendorfer CA, Kyne PM (2009) Limited potential to recover from overfishing raises concerns for deep-sea sharks, rays and chimaeras. Environ Conserv 36:97–103
Simpfendorfer CA, Chin A, Kyne P, Rigby C, Sherman S, White W (2019) Shark futures: a report card for Australia's sharks. Fisheries Research and Development Corporation, Canberra, ACT.
Speed C, Meekan M, Field I, McMahon C, Abrantes K, Bradshaw C (2012) Trophic ecology of reef sharks determined using stable isotopes and telemetry. Coral Reefs 31:357–367
Stevens JD, Bonfil R, Dulvy NK, Walker PA (2000) The effects of fishing on sharks, rays, and chimaeras (chondrichthyans), and the implications for marine ecosystems. ICES J Mar Sci 57:476–494
Valls M, Quetglas A, Ordines F, Moranta J (2011) Feeding ecology of demersal elasmobranchs from the shelf and slope off the Balearic Sea (western Mediterranean). Sci Mar 75:633–639
Valls M, Rueda L, Quetglas A (2017) Feeding strategies and resource partitioning among elasmobranchs and cephalopods in Mediterranean deep-sea ecosystems. Deep Sea Res I 128:28–41
Vaudo J, Heithaus M (2011) Dietary niche overlap in a nearshore elasmobranch mesopredator community. Mar Ecol Prog Ser 425:247–260
Webster MS (2004) Density dependence via intercohort competition in a coral-reef fish. Ecology 85:986–994
Wilga CAD, Diniz SE, Steele PR, Sudario-Cook J, Dumont ER, Ferry LA (2016) Ontogeny of feeding mechanics in smoothhound sharks: morphology and cartilage stiffness. Integr Comp Biol 56:442–448
Yemisken E, Navarro J, Forero M, Megalofonou P, Eryilmaz L (2019) Trophic partitioning between abundant demersal sharks coexisting in the North Aegean Sea. J Mar Biol Assoc UK 99:1213–1219

Editorial responsibility: Robert Suryan, Juneau, Alaska, USA

Submitted: May 31, 2019; Accepted: December 16, 2019
Proofs received from author(s): February 5, 2020